Network Localization Cramér–Rao Bounds for General Measurement Models

Panos N. Alevizos, *Student Member, IEEE,* and Aggelos Bletsas, *Senior Member, IEEE*.

***Abstract*—A closed-form Cramér-Rao bound (CRB) for general multi-modal measurements is derived for D-dimensional network localization ($D \in \{2,3\}$). Links are asymmetric and the measurements among neighboring nodes are non-reciprocal depending on an arbitrary differentiable function of their position difference, subject to additive Gaussian noise (with variance that may depend on distance). The provided bound incorporates network connectivity and could be applied for a wide range of typical, unimodal ranging measurement methods (e.g., angle-of-arrival *or* time-of-arrival *or* signal strength with directional antennas) or multi-modal methods (e.g., simultaneous use of unimodal ranging measurements). It was interesting to see that for specific network connectivity, MSE performance of various different ranging measurement methods coincide, while performance of network localization algorithms is clearly sensitive on network connectivity.**

***Index Terms*—Estimation theory, Cramer-Rao bounds.**

I. Introduction

In network localization [1], [2], agents with unknown location exchange measurements with reference anchors (non-cooperative localization) and other neighboring agents (cooperative localization). Measurements of relative location and distance can be quantified by a variety of metrics, such as received signal strength (RSS) or time-of-arrival (ToA) [1], [3], angle-of-arrival (AoA) [4], [5] or combination [6].

Performance of any localization algorithm usually employs the mean squared-error (MSE) metric, which for unbiased deterministic estimators, is lower-bounded by the Cramér-Rao bound (CRB) [7]. However, prior art has derived CRB formulas for specific measurement setups. For instance, work in [1] offered CRB for two-dimensional (2D) cooperative localization with ToA [8] or RSS-based measurements. Related work [9] has offered 2D non-cooperative localization CRB with hybrid ToA and RSS, while work in [10] offered performance bounds for 2D noncooperative localization with ToA and AoA. It is also worth mentioning that reciprocity in distance-based measurements is typically assumed, which may not hold in practice, given that measuring apparatus at different nodes exhibit independent noise levels. CRB including multi-modal measurements—where more than one type of measurements may be simultaneously offered—is typically not covered in the existing network localization prior art, apart from special cases. Seminal work in [11] offered MSE lower bound expressions, derived directly from exchanged signal waveforms and other physical layer-related information, such as multi-path profile or parameters relevant to the channel statistics; extension to cooperative case is given in [12]. Related applications can be found in [13] and references therein.

This work offers closed-form CRB for D-dimensional network (cooperative or not) localization ($D \in \{2,3\}$), covering multi-modal ranging measurements, asymmetric links, non-reciprocal measurements, and studies the impact of network connectivity on localization. Distance dependence in the variance of ranging error measurements can be also modeled. Differentiable functions, modeling a large class of ranging methods are employed. *Notation*: $\mathbb{1}_A$ denotes the indicator function of statement A, which is one if A is true and zero, otherwise; $\mathsf{tr}(\cdot)$ is the trace operator.

This research has been co-financed by the European Union (European Social Fund-ESF) and Greek national funds through the Operational Program Education and Lifelong Learning of the National Strategic Reference Framework (NSRF) - Research Funding Program: Thales. Investing in knowledge society through the European Social Fund.

The authors are with the Telecom Laboratory, School of Electronic and Computer Engineering, Technical University of Crete, Chania 73100, Greece, (e-mail: palevizos@isc.tuc.gr and aggelos@telecom.tuc.gr).

II. System Model

The network consists of N agents with unknown locations, indexed by set $\mathcal{N}_{\rm g} \triangleq \{1, 2, \ldots, N\}$ and L anchors with a priori known coordinates (across the entire network), indexed by set $\mathcal{N}_{\rm an} \triangleq \{N+1, N+2, \ldots, N+L\}$. The set of all network nodes is denoted by $\mathcal{H} \triangleq \mathcal{N}_{\rm g} \cup \mathcal{N}_{\rm an}$ and for D-dimensional localization, the coordinates of node $i \in \mathcal{H}$ are represented by vector $\mathbf{x}_i = \left[x_{i,1}\ x_{i,2}\ \ldots\ x_{i,D}\right]^\top \in \mathbb{R}^D$. Connectivity matrix $\mathbf{A}$ is defined with elements $A_{i,j} = 1$ ($A_{i,j} = 0$) if node i can (cannot) receive measurements from node j, $\forall i,j \in \mathcal{H}$ and $A_{i,i} = 0$, $\forall i \in \mathcal{H}$. In other words, the ith row of $\mathbf{A}$ indicates the nodes that can send measurements to node i; the set of all these nodes can be written as $\mathcal{H}(i) = \{j \in \mathcal{H} : A_{i,j} = 1\}$. For more flexible modeling, $A_{i,j} \neq A_{j,i}$ in general, i.e., connectivity between terminals may be asymmetric; i may receive measurements from j, while j may not receive measurements from i. The set of directed (measurement connectivity) edges is defined as $\mathcal{G} \triangleq \{(i,j) : i \in \mathcal{H},\ j \in \mathcal{H}(i)\} = \left\{(i,j) \in \mathcal{H}^2 : A_{i,j} = 1\right\}$ and notice that $(i,j) \in \mathcal{G}$ does not necessarily mean that $(j,i) \in \mathcal{G}$. Thus, any type of network connectivity can be explicitly modeled. It is further assumed that all node positions are distinct.

In network localization, agents exchange measurements with other neighboring nodes (agents or anchors) for estimation of the unknown (agent) coordinates $\{\mathbf{x}_n\}_{n \in \mathcal{N}_{\rm g}}$, using set of measurements $\mathbf{Y} \triangleq \left\{y_{i \leftarrow j}^{(m)} : (i,j) \in \mathcal{G},\ m \in \mathcal{M}\right\}$. Set $\mathcal{M} = \{1, 2, \ldots, M\}$ denotes the type of measurements for the pair (i,j), e.g., ToA ($m = 1$), RSS ($m = 2$), AoA ($m = 3$) or other. Specifically, node $i \in \mathcal{H}$ conducts measurement $y_{i \leftarrow j}^{(m)}$ of type m by receiving signal transmitted from neighboring node $j \in \mathcal{H}(i)$, resulting to ranging measurement given by:

$$y_{i \leftarrow j}^{(m)} \triangleq \mathsf{p}_{i \leftarrow j}^{(m)}\left(\mathbf{x}_i, \mathbf{x}_j\right) + \sqrt{\mathsf{h}_{ij}^{(m)}\left(\mathsf{d}_{ij}\right)}\ w_{i \leftarrow j}^{(m)}, \tag{1}$$

with function $\mathsf{p}_{i \leftarrow j}^{(m)}\left(\mathbf{x}_i, \mathbf{x}_j\right) \triangleq \mathsf{g}_{ij}^{(m)}\left(\mathsf{d}_{ij}\right) + \mathsf{v}_{i \leftarrow j}^{(m)}\left(\mathbf{x}_i, \mathbf{x}_j\right)$ and $\mathsf{d}_{ij} \triangleq \|\mathbf{x}_i - \mathbf{x}_j\|$; it is emphasized that $y_{i \leftarrow j}^{(m)} \neq y_{j \leftarrow i}^{(m)}$ in general, even for symmetric connectivity, e.g., due to independent noise levels at different receivers; thus, $\left\{w_{i\leftarrow j}^{(m)} : (i,j) \in \mathcal{G},\ m \in \mathcal{M}\right\}$ are independent, non-identically distributed (i.n.i.d.), zero-mean Gaussian random variables of variance $\left(\sigma_{i\leftarrow j}^{(m)}\right)^2$. For all $(i,j) \in \mathcal{G}$, $m \in \mathcal{M}$, functions $\mathsf{g}_{ij}^{(m)} : \mathbb{R}_+ \longrightarrow \mathbb{R}$ and $\mathsf{h}_{ij}^{(m)} : \mathbb{R}_+ \longrightarrow \mathbb{R}_+$ are assumed differentiable over positive reals and depend solely on d_{ij}, while $\mathsf{v}_{i\leftarrow j}^{(m)} : \mathbb{R}^{2D} \longrightarrow \mathbb{R}$ depends solely on $\mathbf{x}_i - \mathbf{x}_j$ (i.e., $\mathsf{v}_{i\leftarrow j}^{(m)}(\mathbf{x}_i,\mathbf{x}_j) = \widetilde{\mathsf{v}}_{i\leftarrow j}^{(m)}(\mathbf{x}_i - \mathbf{x}_j)$ for some suitable function $\widetilde{\mathsf{v}}_{i\leftarrow j}^{(m)} : \mathbb{R}^D \longrightarrow \mathbb{R}$) and is also assumed differentiable over a neighborhood of $(\mathbf{x}_i,\mathbf{x}_j)$. It can be shown that $\nabla_{\mathbf{x}_i}\mathsf{v}_{i\leftarrow j}^{(m)}(\mathbf{x}_i,\mathbf{x}_j) = -\nabla_{\mathbf{x}_j}\mathsf{v}_{i\leftarrow j}^{(m)}(\mathbf{x}_i,\mathbf{x}_j)$. For each (directed) link $(i,j) \in \mathcal{G}$ and measurement type $m \in \mathcal{M}$, one available measurement is assumed. Specific examples from practice follow.

Examples: For ToA ranging measurements, $\mathsf{h}_{ij}^{(1)}(\cdot) = 1$, $\mathsf{v}_{i\leftarrow j}^{(1)}(\cdot) = 0$, $\mathsf{g}_{ij}^{(1)}(\mathsf{d}_{ij}) = \frac{\mathsf{d}_{ij}}{\mathtt{c}} + \mathtt{b}_{ij}$, $\mathtt{c}$ denotes the signal propagation velocity and $\mathtt{b}_{ij}$ models a bias term accounting for possible non-light-of-sight (NLOS) effects.

For RSS ranging measurements with omnidirectional antennas, $\mathsf{g}_{ij}^{(2)}(\mathsf{d}_{ij}) = P_{ij} - 10\nu_{ij}\mathsf{log}_{10}\left(\frac{\mathsf{d}_{ij}}{d_{0,ij}}\right)$, where ν_{ij} is the path-loss exponent (PLE) between nodes i and j and P_{ij} is the known received power at a short reference distance $d_{0,ij}$.

For RSS ranging measurements with directional antennas, function $\mathsf{v}_{i\leftarrow j}^{(2)}$ is also added in $\mathsf{p}_{i\leftarrow j}^{(2)}$, modeling the gain $\mathsf{G}_j^{\mathrm{Tx}}$ of node's j transmit antenna and gain $\mathsf{G}_i^{\mathrm{Rx}}$ of node's i receive antenna (in dB). Specifically for 2D, $\mathsf{v}_{i\leftarrow j}^{(2)}\left(\mathbf{x}_i,\mathbf{x}_j\right) = 10\mathsf{log}_{10}\left(\mathsf{G}_j^{\mathrm{Tx}}(\phi_{i\leftarrow j})\,\mathsf{G}_i^{\mathrm{Rx}}(\phi_{j\leftarrow i})\right)$, where phase $\phi_{i\leftarrow j} \triangleq \mathsf{tan}_2^{-1}\left(\frac{x_{i,2}-x_{j,2}}{x_{i,1}-x_{j,1}}\right)$ when $\phi_{i\leftarrow j} \in [0,\pi)$, and $\phi_{i\leftarrow j} \triangleq 2\pi + \mathsf{tan}_2^{-1}\left(\frac{x_{i,2}-x_{j,2}}{x_{i,1}-x_{j,1}}\right)$ when $\phi_{i\leftarrow j} \in [\pi,2\pi)$, with function $\mathsf{tan}_2^{-1}\left(\frac{y}{x}\right) \triangleq \mathsf{atan2}(y,x)$, and $\mathsf{atan2}(y,x) \in [-\pi,\pi]$ as defined in [14, Eq. (5.22)]; such definition offers $\phi_{i\leftarrow j}$ ranging in $[0,2\pi)$ (as opposed to classic atan, which is limited to $[-\pi/2,\pi/2]$) and offers a differentiable $\phi_{i\leftarrow j}$. For 3D, $\mathsf{v}_{i\leftarrow j}^{(2)}\left(\mathbf{x}_i,\mathbf{x}_j\right) = 10\mathsf{log}_{10}\left(\mathsf{G}_j^{\mathrm{Tx}}(\phi_{i\leftarrow j},\theta_{i\leftarrow j})\,\mathsf{G}_i^{\mathrm{Rx}}(\phi_{j\leftarrow i},\theta_{j\leftarrow i})\right)$, where $\theta_{i\leftarrow j} = \mathsf{cos}^{-1}\left(\frac{x_{i,3}-x_{j,3}}{\|\mathbf{x}_i-\mathbf{x}_j\|}\right) \in (0,\pi)$.

As a simple 2D example, consider dipole antennas placed parallel to the x-axis [15]. Due to symmetry of the dipole directivity pattern, $\mathsf{v}_{i\leftarrow j}^{(2)}\left(\mathbf{x}_i,\mathbf{x}_j\right)$ is given by:

$$\begin{cases} 20\mathsf{log}_{10}\left(1.67\mathsf{cos}^3\left(\phi_{i\leftarrow j}\right)\right), & \phi_{i\leftarrow j} \in \left[0,\frac{\pi}{2}\right)\cup\left(\frac{3\pi}{2},2\pi\right) \\ 20\mathsf{log}_{10}\left(-1.67\mathsf{cos}^3\left(\phi_{i\leftarrow j}\right)\right), & \phi_{i\leftarrow j} \in \left(\frac{\pi}{2},\frac{3\pi}{2}\right). \end{cases} \tag{2}$$

For a simple 3D example, consider the 3D directivity pattern of dipoles vertical to x-y plane that depends solely on $\theta_{i\leftarrow j}$ [15]. Due to symmetry, function $\mathsf{v}_{i\leftarrow j}^{(2)}\left(\mathbf{x}_i,\mathbf{x}_j\right)$ can be simplified to:

$$\mathsf{v}_{i\leftarrow j}^{(2)}\left(\mathbf{x}_i,\mathbf{x}_j\right) = 20\mathsf{log}_{10}\left(1.67\mathsf{sin}^3\left(\theta_{i\leftarrow j}\right)\right), \tag{3}$$

with $\theta_{i\leftarrow j} \in (0,\pi)$.[1] It is worth noting that in RSS ranging measurements, standard deviation (in dB) may depend on distance and thus, $\mathsf{h}_{ij}^{(2)}(\cdot) \neq 1$ could be also adopted.

[1] Notice that due to the antenna reciprocity theorem, $\mathsf{v}_{i\leftarrow j}^{(2)}(\cdot) = \mathsf{v}_{j\leftarrow i}^{(2)}(\cdot)$; the adopted notation assists clarity regarding which is the transmitting and which is the receiving antenna and network node.

Finally, the 2D AoA measurement model is given by $\mathsf{h}_{ij}^{(3)}(\cdot) = 1$ and $\mathsf{p}_{i\leftarrow j}^{(3)}(\cdot) = \mathsf{v}_{i\leftarrow j}^{(3)}(\cdot)$ with $\mathsf{v}_{i\leftarrow j}^{(3)}\left(\mathbf{x}_i,\mathbf{x}_j\right) = \phi_{i\leftarrow j}$.

III. Cramér-Rao Bound

Vector $\mathbf{x} = \left[\mathbf{x}_{\mathrm{g}}^\top\ \mathbf{x}_{\mathrm{an}}^\top\right]^\top \in \mathbb{R}^{D(N+L)}$ is defined, where $\mathbf{x}_{\mathrm{g}} = \{\mathbf{x}_n\}_{n\in\mathcal{N}_{\mathrm{g}}}$ and $\mathbf{x}_{\mathrm{an}} = \{\mathbf{x}_l\}_{l\in\mathcal{N}_{\mathrm{an}}}$ are associated with agent and anchor positions, respectively. From Eq. (1), measurement at node i (due to transmission from neighboring node j) is distributed according to:

$$y_{i\leftarrow j}^{(m)};\mathbf{x}_i,\mathbf{x}_j \sim \mathcal{N}\left(\mathsf{p}_{i\leftarrow j}^{(m)}\left(\mathbf{x}_i,\mathbf{x}_j\right),\mathsf{h}_{ij}^{(m)}\left(\mathsf{d}_{ij}\right)\left(\sigma_{i\leftarrow j}^{(m)}\right)^2\right), \tag{4}$$

and is independent from the rest of the measurements $\mathbf{Y}\backslash\left\{y_{i\leftarrow j}^{(m)}\right\}$. Thus, the joint log-likelihood distribution of measurements $\mathbf{Y}$ is expressed as:

$$\mathsf{ln}[f(\mathbf{Y};\mathbf{x})] = \sum_{i\in\mathcal{H}}\sum_{j\in\mathcal{H}(i)}\sum_{m\in\mathcal{M}}\underbrace{\mathsf{ln}\left[f\left(y_{i\leftarrow j}^{(m)};\mathbf{x}_i,\mathbf{x}_j\right)\right]}_{\lambda_{i\leftarrow j}^{(m)}}. \tag{5}$$

The Fisher information matrix (FIM) depends on connectivity and location of all nodes (agents or anchors) and is denoted as $\mathbf{J}(\mathbf{x}_{\mathrm{g}},\mathbf{x}_{\mathrm{an}},\mathcal{G})$; it is associated with $f(\mathbf{Y};\mathbf{x})$ and unknown parameters $\mathbf{x}_{\mathrm{g}}$, and is given by:

$$\mathbf{J}(\mathbf{x}_{\mathrm{g}},\mathbf{x}_{\mathrm{an}},\mathcal{G}) = \mathbb{E}_{\mathbf{Y};\mathbf{x}}\left[\nabla_{\mathbf{x}_{\mathrm{g}}}\mathsf{ln}[f(\mathbf{Y};\mathbf{x})]\,\nabla_{\mathbf{x}_{\mathrm{g}}}^\top\mathsf{ln}[f(\mathbf{Y};\mathbf{x})]\right]. \tag{6}$$

FIM in (6) can be equivalently written as [7]:

$$\mathbf{J} \equiv \mathbf{J}(\mathbf{x}_{\mathrm{g}},\mathbf{x}_{\mathrm{an}},\mathcal{G}) = \begin{bmatrix} \mathbf{J}_{1,1} & \cdots & \mathbf{J}_{1,N} \\ \vdots & \ddots & \vdots \\ \mathbf{J}_{N,1} & \cdots & \mathbf{J}_{N,N} \end{bmatrix}, \tag{7}$$

where for $n,k \in \mathcal{N}_{\mathrm{g}}$,

$$\mathbf{J}_{n,k} = \mathbb{E}_{\mathbf{Y};\mathbf{x}}\left[\nabla_{\mathbf{x}_n}\mathsf{ln}[f(\mathbf{Y};\mathbf{x})]\,\nabla_{\mathbf{x}_k}^\top\mathsf{ln}[f(\mathbf{Y};\mathbf{x})]\right] \tag{8}$$

is a $D \times D$ matrix. The directed node ID pairs in the two outermost summations of Eq. (5) involving an agent $n \in \mathcal{N}_{\mathrm{g}}$, are given by the following set:

$$\mathcal{A}(n) \triangleq \bigcup_{j\in\mathcal{H}}\left\{(n,j) : A_{n,j} = 1\right\} \cup \left\{(j,n) : A_{j,n} = 1\right\}. \tag{9}$$

The set above incorporates all (directed) links in the network where agent n is involved either as transmitter or receiver, during ranging measurements.

Regularity conditions of $f\left(y_{i\leftarrow j}^{(m)};\mathbf{x}_i,\mathbf{x}_j\right)$ for each $(i,j) \in \mathcal{G}$ will be utilized [7], i.e., for any $n \in \mathcal{N}_{\mathrm{g}}$ and any $(i,j) \in \mathcal{A}(n)$,

$$\mathbb{E}_{\mathbf{Y};\mathbf{x}}\left[\nabla_{\mathbf{x}_n}\lambda_{i\leftarrow j}^{(m)}\right] = \mathbf{0}_D,\ \text{for a.e. } \mathbf{x}_n \in \mathbb{R}^D. \tag{11}$$

Applying $\nabla_{\mathbf{x}_n}$ in (5) and eliminating the terms $\lambda_{i\leftarrow j}^{(m)}$ that do not depend on $\mathbf{x}_n$ offers:

$$\nabla_{\mathbf{x}_n}\mathsf{ln}[f(\mathbf{Y};\mathbf{x})] \overset{(9)}{=} \sum_{m\in\mathcal{M}}\sum_{(i,j)\in\mathcal{A}(n)}\nabla_{\mathbf{x}_n}\lambda_{i\leftarrow j}^{(m)}. \tag{12}$$

For any $n \in \mathcal{N}_{\mathrm{g}}$ and any $(i,j) \in \mathcal{A}(n)$, $(i',j') \in \mathcal{A}(n)$ and $m,m' \in \mathcal{M}$, measurements $y_{i\leftarrow j}^{(m)}$ and $y_{i'\leftarrow j'}^{(m')}$ are independent, unless $m = m'$, $i = i'$, and $j = j'$. Thus, by the regularity conditions of Eq. (11), $\mathbb{E}_{\mathbf{Y};\mathbf{x}}\left[\nabla_{\mathbf{x}_n}\lambda_{i\leftarrow j}^{(m)}\nabla_{\mathbf{x}_n}^\top\lambda_{i'\leftarrow j'}^{(m')}\right]$ is non-zero only if $m = m'$, $i = i'$, $j = j'$ for any $(i,j) \in \mathcal{A}(n)$. Using the

$$\mathbf{J}_{n,k}=\begin{cases}\sum\limits_{m\in\mathcal{M}}\left(\sum\limits_{(i,j)\in\mathcal{A}(n)}\left(\frac{\left[\dot{\mathsf{h}}_{ij}^{(m)}(\|\mathbf{x}_i-\mathbf{x}_j\|)\right]^2(\mathbf{x}_i-\mathbf{x}_j)(\mathbf{x}_i-\mathbf{x}_j)^\top}{2\ \left[\mathsf{h}_{ij}^{(m)}(\|\mathbf{x}_i-\mathbf{x}_j\|)\right]^2\ \|\mathbf{x}_i-\mathbf{x}_j\|^2}\right.\right.\\ \left.\left.+\frac{\left(\frac{\left[\dot{\mathsf{g}}_{ij}^{(m)}(\|\mathbf{x}_i-\mathbf{x}_j\|)\right](\mathbf{x}_i-\mathbf{x}_j)}{\|\mathbf{x}_i-\mathbf{x}_j\|}+\nabla_{\mathbf{x}_n}\mathsf{v}_{i\leftarrow j}^{(m)}(\mathbf{x}_i,\mathbf{x}_j)\right)\left(\frac{\left[\dot{\mathsf{g}}_{ij}^{(m)}(\|\mathbf{x}_i-\mathbf{x}_j\|)\right](\mathbf{x}_i-\mathbf{x}_j)^\top}{\|\mathbf{x}_i-\mathbf{x}_j\|}+\nabla_{\mathbf{x}_n}^\top\mathsf{v}_{i\leftarrow j}^{(m)}(\mathbf{x}_i,\mathbf{x}_j)\right)}{\left(\sigma_{i\leftarrow j}^{(m)}\right)^2\ \mathsf{h}_{ij}^{(m)}(\|\mathbf{x}_i-\mathbf{x}_j\|)}\right)\right), & n=k\\[2ex] -\sum\limits_{m\in\mathcal{M}}\left(\sum\limits_{\substack{(i,j)\in\\(n,k)\cup(k,n)}}\mathbb{1}_{(i,j)\in\mathcal{G}}\left(\frac{\left[\dot{\mathsf{h}}_{ij}^{(m)}(\|\mathbf{x}_i-\mathbf{x}_j\|)\right]^2(\mathbf{x}_i-\mathbf{x}_j)(\mathbf{x}_i-\mathbf{x}_j)^\top}{2\ \left[\mathsf{h}_{ij}^{(m)}(\|\mathbf{x}_i-\mathbf{x}_j\|)\right]^2\ \|\mathbf{x}_i-\mathbf{x}_j\|^2}\right.\right.\\ \left.\left.+\frac{\left(\frac{\left[\dot{\mathsf{g}}_{ij}^{(m)}(\|\mathbf{x}_i-\mathbf{x}_j\|)\right](\mathbf{x}_i-\mathbf{x}_j)}{\|\mathbf{x}_i-\mathbf{x}_j\|}+\nabla_{\mathbf{x}_n}\mathsf{v}_{i\leftarrow j}^{(m)}(\mathbf{x}_i,\mathbf{x}_j)\right)\left(\frac{\left[\dot{\mathsf{g}}_{ij}^{(m)}(\|\mathbf{x}_i-\mathbf{x}_j\|)\right](\mathbf{x}_i-\mathbf{x}_j)^\top}{\|\mathbf{x}_i-\mathbf{x}_j\|}+\nabla_{\mathbf{x}_n}^\top\mathsf{v}_{i\leftarrow j}^{(m)}(\mathbf{x}_i,\mathbf{x}_j)\right)}{\left(\sigma_{i\leftarrow j}^{(m)}\right)^2\ \mathsf{h}_{ij}^{(m)}(\|\mathbf{x}_i-\mathbf{x}_j\|)}\right)\right), & n\neq k.\end{cases} \quad (16)$$

above and substituting Eq. (12) in (8) for $k=n$, the diagonal blocks in (7) can be calculated as:

$$\mathbf{J}_{n,n}=\sum_{m\in\mathcal{M}}\sum_{(i,j)\in\mathcal{A}(n)}\mathbb{E}_{\mathbf{Y};\mathbf{x}}\left[\nabla_{\mathbf{x}_n}\lambda_{i\leftarrow j}^{(m)}\nabla_{\mathbf{x}_n}^\top\lambda_{i\leftarrow j}^{(m)}\right]. \quad (13)$$

Similarly, due to the regularity conditions, for any $k,n\in\mathcal{N}_{\mathrm{g}}$, with $k\neq n$, $\mathbb{E}_{\mathbf{Y};\mathbf{x}}\left[\nabla_{\mathbf{x}_n}\lambda_{i\leftarrow j}^{(m)}\nabla_{\mathbf{x}_k}^\top\lambda_{i'\leftarrow j'}^{(m')}\right]$ is a nonzero matrix only if $k\in\mathcal{H}(n)$, $m=m'$, $i=i'=n$, $j=j'=k$, or only if $n\in\mathcal{H}(k)$, $m=m'$, $i=i'=k$, $j=j'=n$. Thus, after some algebra, the non-diagonal blocks in Eq. (7) can be expressed as:

$$\mathbf{J}_{n,k}=\sum_{m\in\mathcal{M}}\sum_{\substack{(i,j)\in\\(n,k)\cup(k,n)}}\mathbb{1}_{(i,j)\in\mathcal{G}}\,\mathbb{E}_{\mathbf{Y};\mathbf{x}}\left[\nabla_{\mathbf{x}_n}\lambda_{i\leftarrow j}^{(m)}\nabla_{\mathbf{x}_k}^\top\lambda_{i\leftarrow j}^{(m)}\right]. \quad (14)$$

It is also noted that for any $n\in\mathcal{N}_{\mathrm{g}}$ and $k\in\mathcal{H}(n)$,

$$\begin{aligned}\mathbb{E}_{\mathbf{Y};\mathbf{x}}\left[\nabla_{\mathbf{x}_n}\lambda_{n\leftarrow k}^{(m)}\nabla_{\mathbf{x}_n}^\top\lambda_{n\leftarrow k}^{(m)}\right]&\overset{(a)}{=}-\mathbb{E}_{\mathbf{Y};\mathbf{x}}\left[\nabla_{\mathbf{x}_n}\lambda_{n\leftarrow k}^{(m)}\nabla_{\mathbf{x}_k}^\top\lambda_{n\leftarrow k}^{(m)}\right]\\ &\overset{(b)}{=}\frac{\left(\nabla_{\mathbf{x}_n}\mathsf{p}_{n\leftarrow k}^{(m)}(\mathbf{x}_n,\mathbf{x}_k)\right)\left(\nabla_{\mathbf{x}_n}^\top\mathsf{p}_{n\leftarrow k}^{(m)}(\mathbf{x}_n,\mathbf{x}_k)\right)}{\mathsf{h}_{nk}^{(m)}(\mathsf{d}_{nk})\left(\sigma_{n\leftarrow k}^{(m)}\right)^2}+\\ &\quad+\frac{\nabla_{\mathbf{x}_n}\mathsf{h}_{nk}^{(m)}(\mathsf{d}_{nk})\nabla_{\mathbf{x}_n}^\top\mathsf{h}_{nk}^{(m)}(\mathsf{d}_{nk})}{2\ \left[\mathsf{h}_{nk}^{(m)}(\mathsf{d}_{nk})\right]^2}.\end{aligned} \quad (15)$$

Equality (a) holds due to $\nabla_{\mathbf{x}_n}\lambda_{n\leftarrow k}^{(m)}=-\nabla_{\mathbf{x}_k}\lambda_{n\leftarrow k}^{(m)}$; the latter holds because $\lambda_{n\leftarrow k}^{(m)}$ is a function that depends on the difference $\mathbf{x}_n-\mathbf{x}_k$, stemming directly from Eq. (1) and the assumptions of Sec. II. Equality (b) stems from the fact that all functions are differentiable near $(\mathbf{x}_n,\mathbf{x}_k)$ and [7, Eq. (3.31)].

Substituting Eq. (15) in (13) and (14), we obtain the expression in (16) at the top of the page. In (16), we also employ the chain rule of differentiation and $\nabla_{\mathbf{x}_n}\mathsf{d}_{nk}=\frac{\mathbf{x}_n-\mathbf{x}_k}{\|\mathbf{x}_n-\mathbf{x}_k\|}$, which is properly defined due to the distinct node positions assumption. Notation $\dot{\mathsf{g}}_{nk}^{(m)}(\mathsf{d}_{nk})$ and $\dot{\mathsf{h}}_{nk}^{(m)}(\mathsf{d}_{nk})$ denotes the first derivative of $\mathsf{g}_{nk}^{(m)}(\cdot)$ and $\mathsf{h}_{nk}^{(m)}(\cdot)$, respectively, evaluated at point $\mathsf{d}_{nk}=\|\mathbf{x}_n-\mathbf{x}_k\|$.

The MSE of any unbiased deterministic estimator $\widehat{\mathbf{x}}_n$, of the nth agent position is lower bounded by:

$$\mathbb{E}_{\mathbf{Y};\mathbf{x}}\left[\|\widehat{\mathbf{x}}_n-\mathbf{x}_n\|^2\right]\geq\mathsf{tr}\left(\mathbf{J}_{n,n}^{-1}\right), \quad (17)$$

where $\mathbf{J}_{n,n}^{-1}$ is the nth diagonal $D\times D$ matrix block of $\mathbf{J}^{-1}$.

A. FIM Evaluation for Different Measurement Models

To see the utility of Eq. (16), some application examples follow:

- ToA: $\dot{\mathsf{g}}_{ij}^{(1)}(\mathsf{d}_{ij})=\frac{1}{\mathsf{c}}$ and $\nabla_{\mathbf{x}_i}\mathsf{v}_{i\leftarrow j}^{(1)}\left(\mathbf{x}_i,\mathbf{x}_j\right)=\mathbf{0}_D$.
- 2D RSS, according to Eq. (2): $\dot{\mathsf{g}}_{ij}^{(2)}(\mathsf{d}_{ij})=\frac{-10\nu_{ij}}{\ln(10)\mathsf{d}_{ij}}$ and

$$\nabla_{\mathbf{x}_i}\mathsf{v}_{i\leftarrow j}^{(2)}\left(\mathbf{x}_i,\mathbf{x}_j\right)=\begin{bmatrix}\frac{60(x_{i,2}-x_{j,2})^2}{\ln(10)\ \mathsf{d}_{ij}^2(x_{i,1}-x_{j,1})}\\ \frac{-60(x_{i,2}-x_{j,2})}{\ln(10)\ \mathsf{d}_{ij}^2}\end{bmatrix}. \quad (18)$$

- 3D RSS, according to Eq. (3): $\dot{\mathsf{g}}_{ij}^{(2)}(\mathsf{d}_{ij})=\frac{-10\nu_{ij}}{\ln(10)\mathsf{d}_{ij}}$ and

$$\nabla_{\mathbf{x}_i}\mathsf{v}_{i\leftarrow j}^{(2)}\left(\mathbf{x}_i,\mathbf{x}_j\right)=\frac{60}{\ln(10)\ \mathsf{d}_{ij}^2}\begin{bmatrix}\frac{(x_{i,3}-x_{j,3})^2(x_{i,1}-x_{j,1})}{\left(\mathsf{d}_{ij}^2-(x_{i,3}-x_{j,3})^2\right)}\\ \frac{(x_{i,3}-x_{j,3})^2(x_{i,2}-x_{j,2})}{\left(\mathsf{d}_{ij}^2-(x_{i,3}-x_{j,3})^2\right)}\\ -(x_{i,3}-x_{j,3})\end{bmatrix}. \quad (19)$$

- 2D AoA: $\dot{\mathsf{g}}_{ij}^{(3)}(\mathsf{d}_{ij})=0$ and

$$\nabla_{\mathbf{x}_i}\mathsf{v}_{i\leftarrow j}^{(3)}\left(\mathbf{x}_i,\mathbf{x}_j\right)=\begin{bmatrix}\frac{-(x_{i,2}-x_{j,2})}{\mathsf{d}_{ij}^2}\\ \frac{(x_{i,1}-x_{j,1})}{\mathsf{d}_{ij}^2}\end{bmatrix}. \quad (20)$$

With the help of the above and $\nabla_{\mathbf{x}_i}\mathsf{v}_{i\leftarrow j}^{(m)}(\mathbf{x}_i,\mathbf{x}_j)=-\nabla_{\mathbf{x}_j}\mathsf{v}_{i\leftarrow j}^{(m)}(\mathbf{x}_i,\mathbf{x}_j)$, matrix $\mathbf{J}$ is directly calculated.

IV. Numerical Results

Numerical results for 2D and 3D localization are presented, as a function of measurement noise variance, type of ranging measurements (or combination of methods) and connectivity radius (assuming—for conciseness—common connectivity radius r among all terminals). A common measurement noise variance is assumed, i.e., $\sigma_{i\leftarrow j}^{(m)}=\sigma^{(m)}$, $\forall(i,j)\in\mathcal{G}$ and the values for $\sigma^{(m)}$ are taken from real experimental testbeds [1], [2]. In addition, PLE is assumed known i.e., $\nu_{ij}=\nu=$

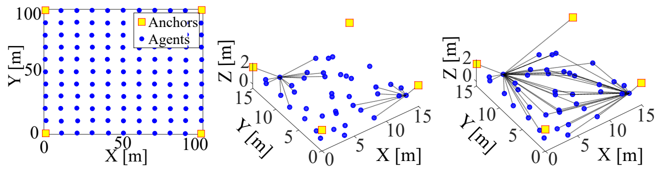

Fig. 1. Left: $N = 117$ agents and $L = 4$ anchors. Middle and right: $N = 40$ agents and $L = 4$ anchors for $r = 7$ and $r = 12$, respectively. Connectivity for two nodes is also depicted in middle and right, for illustration purposes.

2.3, $\forall(i, j) \in \mathcal{G}$ in RSS measurements [2]. The final CRB averaged across all agents is given by $\mathrm{CRB} = \frac{1}{N}\mathrm{tr}\left(\mathbf{J}^{-1}\right)$.

Fig. 2 illustrates the CRB performance for the 2D topology of Fig. 1-left, as a function of communication radius r, across different ranging measurement methods. The RSS measurement model without directionality (line with crosses) has the worst MSE performance. When network nodes are equipped with dipole antennas parallel to the x-axis, the MSE (line with circles) can be further reduced. AoA measurement model (line with x's) further reduces MSE compared to classic RSS for the specific topology, while ToA (diamonds) offers the best MSE across all measurement methods above. Interestingly, exploitation of 2 types of measurements significantly improves MSE performance, as shown in Fig. 2; AoA and RSS could outperform ToA for specific network connectivity, while joint ToA and RSS with dipole antennas can significantly reduce MSE. It is also interesting to see that for specific network connectivity, MSE performance of various different ranging measurement methods coincide. Closed-form FIM calculation of this framework allows simple performance comparisons across different ranging methods *and* network topologies.

Fig. 3 offers results for the 3D topology of Fig. 1-middle and right. RSS offers similar MSE compared to ToA measurements, while RSS with directivity outperforms ToA. That is due to the small distances involved, and thus, the terms not depending on distances dominate in FIM. The proposed CRB was also used to benchmark state-of-the-art network localization algorithms, e.g., MDS-MAP [16], which is a refined version of classic multi-dimensional scaling (MDS), originally designed for full connectivity scenarios, i.e., for large values of r. Fig. 3 shows that for $r \geq 18$, MDS-MAP with ToA reaches CRB. Additionally, it is shown that performance comparison clearly depends on network connectivity. Hopefully, the proposed bound will be used for benchmarking in network localization research.

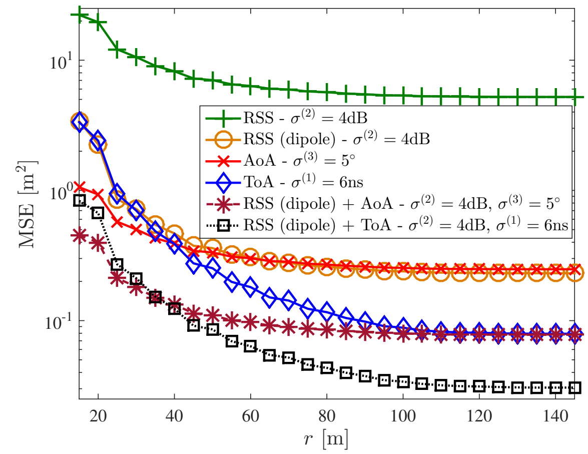

Fig. 2. CRB for Fig. 1-left: Multi-modal ranging measurements improve localization, performance may coincide for specific network connectivity.

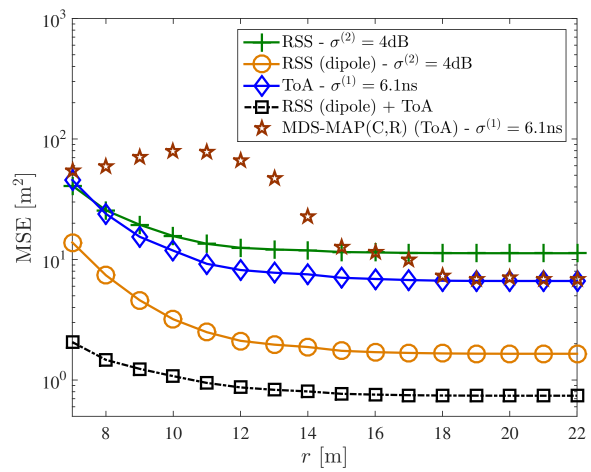

Fig. 3. CRB for 3D topology in Fig. 1-middle and right.

References

[1] N. Patwari, A. O. Hero III, M. Perkins, N. S. Correal, and R. J. O'Dea, "Relative location estimation in wireless sensor networks," *IEEE Trans. Signal Process.*, vol. 51, no. 8, pp. 2137–2148, Aug. 2003.

[2] N. Patwari *et al.*, "Locating the nodes: Cooperative localization in wireless sensor networks," *IEEE Signal Process. Mag.*, vol. 22, no. 4, pp. 54–69, Jul. 2005.

[3] A. Conti, M. Guerra, D. Dardari, N. Decarli, and M. Z. Win, "Network experimentation for cooperative localization," *IEEE J. Sel. Areas Commun.*, vol. 30, no. 2, pp. 467– 475, Feb. 2012.

[4] Y. Zhang, S. Liu, and Z. Jia, "Localization using joint distance and angle information for 3D wireless sensor networks," *IEEE Commun. Lett.*, vol. 16, no. 6, pp. 809–811, Jun. 2012.

[5] D. Niculescu and B. R. Badrinath, "Ad hoc positioning system (APS) using AOA," in *Proc. IEEE Int. Conf. on Computer Communications (Infocom)*, vol. 3, San Francisco, CA, Apr. 2003, pp. 1734–1743.

[6] E. Alimpertis, N. Fasarakis-Hilliard, and A. Bletsas, "Community RF sensing for source localization," *IEEE Wireless Commun. Lett.*, vol. 3, no. 4, pp. 393–396, Aug. 2014.

[7] S. M. Kay, *Fundamentals of Statistical Signal Processing: Estimation Theory*. Upper Saddle River, NJ, USA: Prentice-Hall, Inc., 1993.

[8] C. Chang and A. Sahai, "Cramér-Rao-type bounds for localization," *EURASIP J. Appl. Signal Process.*, vol. 2006, pp. 166–166, Jan. 2006.

[9] A. Catovic and Z. Sahinoglu, "The Cramer-Rao bounds of hybrid TOA/RSS and TDOA/RSS location estimation schemes," *IEEE Commun. Lett.*, vol. 8, no. 10, pp. 626–628, Oct. 2004.

[10] R. L. Moses, D. Krishnamurthy, and R. M. Patterson, "An autocalibration method for unattended ground sensors," in *Proc. IEEE Int. Conf. Acoustics, Speech, and Signal Processing (ICASSP)*, Orlando, FL, 2002, pp. 2941–2944.

[11] Y. Shen and M. Z. Win, "Fundamental limits of wideband localization–part I: A general framework," *IEEE Trans. Inf. Theory*, vol. 56, no. 10, pp. 4956–4980, Oct. 2010.

[12] Y. Shen, H. Wymeersch, and M. Z. Win, "Fundamental limits of wideband localization–part II: Cooperative networks," *IEEE Trans. Inf. Theory*, vol. 56, no. 10, pp. 4981–5000, Oct. 2010.

[13] K. Witrisal *et al.*, "High-Accuracy localization for assisted living: 5G systems will turn multipath channels from foe to friend," *IEEE Signal Process. Mag.*, vol. 33, no. 2, pp. 59–70, Mar. 2016.

[14] S. Thrun, W. Burgard, and D. Fox, *Probabilistic Robotics*. Cambridge, MA: The MIT Press, 2006.

[15] C. Balanis, *Antenna Theory: Analysis and Design*. Wiley, 2012.

[16] Y. Shang, W. Ruml, Y. Zhang, and M. Fromherz, "Localization from connectivity in sensor networks," *IEEE Trans. Parallel Distrib. Syst.*, vol. 15, no. 11, pp. 961–974, Nov. 2004.